Nucleic Acids Research, 2026, **54**, gkag747
https://doi.org/10.1093/nar/gkag747
Synthetic Biology and Bioengineering

Harnessing natural RNA triplex elements found in lncRNAs MALAT1 and NEAT1 for engineering of novel riboswitch platforms

Pierre Gommeringer [1,2,3], Elisabeth Müller [1,2], Sila Köse [1,2], Laura Kayser [3], Mathias F Leber [3,4], Guy Ungerechts [3,4], Dirk M Nettelbeck [3], Jörg S Hartig [1,2,*]

[1]Department of Chemistry, University of Konstanz, 78464 Konstanz, Germany
[2]Konstanz Research School Chemical Biology (Kors-CB), University of Konstanz, 78464 Konstanz, Germany
[3]Clinical Cooperation Unit Virotherapy, German Cancer Research Center (DKFZ), 69120 Heidelberg, Germany
[4]Department of Medical Oncology, Heidelberg University Hospital, National Center for Tumor Diseases (NCT), 69120 Heidelberg, Germany
*To whom correspondence should be addressed. Email: joerg.hartig@uni-konstanz.de

Abstract

Synthetic riboswitches are efficient tools to render gene expression inducible by small molecules. Here, we present a novel riboswitch platform based on RNA triplexes stabilizing non-polyadenylated transcripts while still allowing translation of the respective messenger RNA. By incorporating a tetracycline aptamer, we rendered triplex formation dependent upon the presence of the ligand. The new riboswitch platform was able to induce gene expression up to 25-fold as a standalone switch. Combination of the triplex system with an aptazyme placed into the 5′-UTR achieved a 42-fold induction of gene expression. Further, we were able to exchange the triplex, the aptamer, the maturation platform cleaving off the poly-A tail of the switch platform, and the regulated transgene, demonstrating a high degree of modularity. The new riboswitch platform is designed to function independently of nuclear processes such as transcription and RNA processing, potentially expanding the application of these synthetic riboswitches to strictly cytoplasmic therapeutic RNA vectors.

Graphical abstract

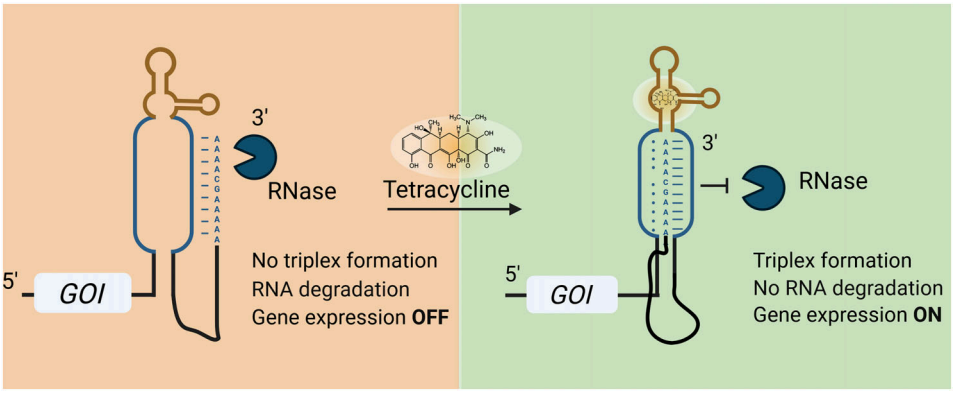

Introduction

Gene therapy as well as basic research have growing needs for systems allowing for temporal control over gene expression in mammalian cells [1]. Synthetic riboswitches are RNA-based tools that can control various steps of gene expression by interacting with small molecule ligands. They have emerged as elegant tools for exogenous control of gene expression triggered via small molecules. Inspired by bacterial riboswitches [2], the field of synthetic biology is developing systems that function in the context of the mammalian cell environments and can be switched in dependence of clinically applicable and FDA-approved small molecules [3, 4]. Synthetic riboswitches are composed of two units: (i) an aptamer, which functions as a sensing domain, and (ii) an expression platform that modulates gene expression. Upon ligand binding, the aptamer undergoes conformational changes, translating the binding event onto the expression platform, resulting in change of gene expression. Synthetic aptamers have been

Received: December 23, 2025. **Revised:** July 6, 2026. **Accepted:** July 8, 2026
© The Author(s) 2026. Published by Oxford University Press.
This is an Open Access article distributed under the terms of the Creative Commons Attribution-NonCommercial License (https://creativecommons.org/licenses/by-nc/4.0/), which permits non-commercial re-use, distribution, and reproduction in any medium, provided the original work is properly cited. For commercial re-use, please contact reprints@oup.com for reprints and translation rights for reprints. All other permissions can be obtained through our RightsLink service via the Permissions link on the article page on our site—for further information please contact journals.permissions@oup.com.

Downloaded from academic.oup.com/nar/article/54/14/gkag747/8742449 by Deutsches Krebsforschungszentrum user on 18 November 2026

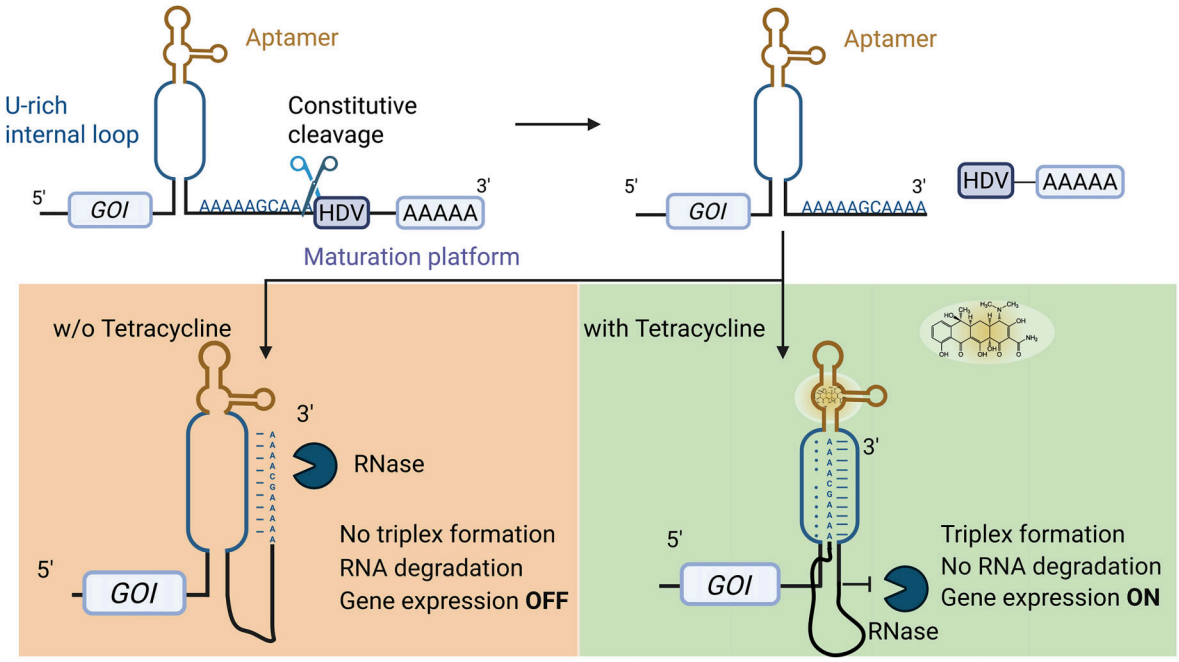

Figure 1. Schematic representation of the RNA triplex called MALAT1 ENE for tetracycline-dependent triplex formation and mRNA stabilization. The poly-A tail is cleaved off by the maturation platform, here an HDV ribozyme. In the absence of tetracycline, the aptamer does not fold into a stable communication module, inhibiting folding of the MALAT1 triplex and stabilization of the mRNA through prevention of RNase-mediated degradation. Tetracycline addition induces triplex formation, leading to mRNA stabilization. Created in BioRender; Gommeringer, P. (2026) https://BioRender.com/j36r7qg.

developed using SELEX approaches [5, 6]. With this method, the cb28 tetracycline-binding aptamer was identified [7, 8] and has since been widely used in the field due to high affinity to its ligand. Systems that are able to induce gene expression (ON) and systems that repress gene expression (OFF) were developed. Although mostly focusing on aptamer-controlled ribozymes (aptazymes) for the development of ON riboswitches [9–12], additional expression platforms have been engineered based on alternative splicing and exon skipping [13–16], occlusion of microRNA (miRNA) target sites [17] and poly-A cleavage sites [18, 19]. While widely researched in the field, most of the described inducible riboswitches only show moderate dynamic ranges, are dependent on the expression of specific miRNAs in the target cells or are dependent on nuclear proteins, limiting the applicability and the modularity of the systems. Hence, there is still need for the development of additional expression platforms that are easy to implement, show robust performances combined with high dynamic ranges and can be modularly adapted.

Long non-coding RNAs (lncRNA) are involved in various cellular processes, including phase separation [20, 21] and gene regulation by miRNA sponging [22]. To address these highly diverse roles, lncRNAs have evolved functional structures, which so far have been understudied but could be exploited for synthetic RNA engineering efforts. Metastasis-associated lung adenocarcinoma transcript 1 (MALAT1) is a nuclear lncRNA [23] associated with various diseases, including cancer [24]. It evolved a non-polyadenylated 3′ end that, instead of a poly-A tail, exhibits an RNA triplex structure [25, 26], also called expression and nuclear retention element (ENE). Its 3′ end is processed via RNAse P recognition of a tRNA-like fold, the MALAT1-associated small cytoplasmic RNA (mascRNA) [27], cleaving off the downstream poly-A tail and resulting in a free 3′ A-rich tract. This 3′-end interacts with a U-rich internal loop to form a RNA triplex structure, protecting the transcript from RNase-mediated degradation [26]. Similar triplex structures have also been characterized in the polyadenylated nuclear RNA of Kaposi's sarcoma-associated herpesvirus (KSHV) [28] and the nuclear enriched abundant transcript 1 (NEAT1) lncRNA [29]. Additional triplex structures have since been identified bioinformatically in all domains of life [30, 31]; however, most of the identified RNAs rely on their poly-A tail to interact with either one or two U-rich internal loops [25, 32].

The MALAT1 and NEAT1 triplexes show unique structural properties. Both their 3′-end A-rich tracts are genomically encoded and released via RNAse P processing of the mascRNA, functioning as the natural maturation platform [27]. This also leads to the release of the A-rich tract that then interacts with a U-rich loop structure. Molecular dynamics simulations have suggested that the U-rich internal loop pre-forms, and the A-rich tract folds onto it in a second step [33]. Additionally, it was shown using isothermal calorimetry that triplex formation is highly dependent upon formation of the U-rich loop and on the stability of the surrounding duplex structures [34]. Since triplex structures prevent RNAse-mediated degradation they can increase the half-life of RNA transcripts [25].

Here, we describe a novel riboswitch platform based on RNA stability elements, namely the MALAT1 ENE and NEAT1 ENE triplexes, working as an ON switch (Fig. 1). While the natural MALAT1 RNA triplex is processed via nuclear RNAse P recognition and cleavage of the mascRNA (Supplementary Fig. S1), we engineered our platform to be matured by a hepatitis delta virus (HDV) ribozyme as previously reported [35]. This allows the riboswitch to function independently of nuclear proteins. Further, we replaced the

Downloaded from academic.oup.com/nar/article/54/14/gkag747/8742449 by Deutsches Krebsforschungszentrum user on 18 November 2026

stable apical stem (Supplementary Fig. S1) with the tetracycline aptamer cb28 [7]. We designed the system in a way that without tetracycline the internal U-rich loop cannot pre-form in the correct conformation leading to the A-rich stretch not being able to fold into a stable RNA triplex structure. The messenger RNA (mRNA) is therefore prone to degradation, since it lacks a protective poly-A tail and the duplex structure being unwound by helicases [36]. In the presence of tetracycline, a suited connecting stem, also called communication module, would allow the U-rich internal loop to pre-form in order to facilitate the A-rich stretch to back-fold and form the stabilizing RNA triplex, thereby inducing gene expression. We demonstrate that the formation of RNA triplexes can be engineered to be dependent on structural rearrangement of guanine and tetracycline aptamers, achieving high induction rates of up to 25-fold. Further, we investigated the modularity of the system by exchanging the open reading frame (ORF), the triplex and the maturation platform. The data show that the triplex-based riboswitch retained inducibility upon exchange of these elements. Our study introduces a promising new riboswitch platform and indicates that further systems with advanced properties can be developed by exploiting lncRNA elements.

Materials and methods

Plasmid construction and cloning

All sequences were introduced into the psiCHECK™-2 vector (Promega) carrying two luciferase genes, the Renilla (hRLuc) and Firefly luciferase (hLuc+). For eGFP measurements mIL12, and mIFNβ enzyme-linked immune-sorbent assay (ELISA), the Renilla luciferase was replaced with the respective gene. The MALAT1 triplex sequence was retrieved from [25] and inserted downstream of the stop codon. Cloning was performed using standard cloning techniques, either via Gibbson assembly (NEB) or overhang polymerase chain reaction (PCR). After successful PCR amplification of the desired constructs, the PCR product was incubated with *DpnI* (NEB) in CutSmart buffer to digest the template and later purified by agarose gel electrophoresis. Recovery was performed either by Zymoclean Gel DNA Recovery Kit (Zymo) or by QIAquick gel purification kit (Qiagen). After ligation with Quick Ligase (NEB) or assembly using Gibson Assembly Master Mix (NEB), and either electrocompetent XL10-Gold *Escherichia coli* (Stratagene) or chemically competent NEB10β *E. coli* (NEB) were transformed. Individual colonies were picked, and plasmids were extracted using either Zyppy plasmid Miniprep kit (Zymo) or QIAprep Spin Miniprep kit (Qiagen). Plasmids were verified to contain the correct sequence by Sanger sequencing at Eurofins Genomics/GATC Biotech or Azenta Genewiz. Sequences used are listed in Supplementary Table S1.

The DNA sequences of the eGFP variants were synthesized by Twist Bioscience. Plasmid encoding murine interferon β was purchased from Sino biologics. Murine single chain interleukin (IL)-12 was fused using a glycine-serine linker according to Lieschke *et al.* [37].

Cell culture

HeLa cells and HEK293 cells were cultured in Dulbecco's modified Eagle's medium (DMEM) + GlutaMAX-I + 10% fetal calf serum (Gibco/Thermo Fisher Scientific). All cells were cultivated at 37°C with 5% CO_2. Prior to transfection, HeLa and HEK293 cells were seeded at densities of 8000 and 10 000 cells per well, respectively, in a 96-well plate, to achieve 60%–70% confluency after 24 h. Transfection was conducted using either Lipofectamine 2000 or Lipofectamine 3000 (Invitrogen) in OptiMEM (Gibco/Thermo Fisher Scientific) according to the manufacturer's protocol. After 4–6 h at 37°C, medium was changed to DMEM containing either tetracycline at indicated concentrations or equal amounts of dimethyl sulfoxide.

Dual luciferase assay

Cells were transfected 24 h before the experiment with the corresponding plasmid and induced 4 h post transfection. Dual-Luciferase Reporter Assays (Promega) were performed using 40 µl of Passive Lysis Buffer in a 96-well plate. After 15 min of incubation at room temperature, 30 µl of lysate were transferred to black 96-well plates. First 30 µl of Luciferase Assay Reagent II was added, followed by Stop & Glo® Reagent. The plate was measured after each addition. Measurements were either performed using a Spark® multimode microplate reader (Tecan) or on an Infinite 200M Pro reader (Tecan) with a settle time of 0 ms and an integration time of 2000 ms. All constructs were measured in technical triplicates in three independent biological experiments. Luciferase data were normalized to the internal control to reduce variation in transfection efficiency. The values were normalized to the mean of the uninduced psiCHECK™-2 control.

eGFP measurement

The eGFP DNA sequence was introduced in the position of the Renilla luciferase in the psiCHECK™-2 plasmid. HeLa $8*10^3$ cells were seeded in black 96-well plates and transfected with the corresponding plasmid or mock-transfected. After 24 h, cells were lysed using 30 µl of Passive Lysis Buffer, and fluorescence was measured at an excitation of 485 nm and an emission of 535 nm, using an integration time of 20 µs and 25 flashes on an Infinite 200M Pro reader (Tecan). Wells were measured in a 4 × 4 square configuration. Firefly luciferase activity was measured as described above. Signals were normalized using the following formula:

$$\text{Relative eGFP signal} = \frac{\text{eGFP}_{\text{construct}} - \text{eGFP}_{\text{Mock}}}{\text{hLuc+}}.$$

Enzyme-linked immune-sorbent assay

Mouse IL-12 p70 DuoSet ELISA kits and Mouse IFN-beta DuoSet ELISA were purchased from R&D Systems for ELISA measurements. Cells were transfected as described above. Supernatants of transfected cells were harvested 24 h post transfection and stored at −80°C until further processing. Plates were coated with the capture antibody overnight at 4°C and blocked for 2 h at room temperature before loading. Samples were incubated overnight at 4°C. After first incubation with the detection antibody for 1 h at room temperature, followed by incubation with HRP (30 min, RT), TMB solution (Thermo Scientific) was added and the reaction was stopped using H_2SO_4. ELISA was measured at 450 nm on an Infinite 200M Pro reader (Tecan).

Downloaded from academic.oup.com/nar/article/54/14/gkag747/8742449 by Deutsches Krebsforschungszentrum user on 18 November 2026

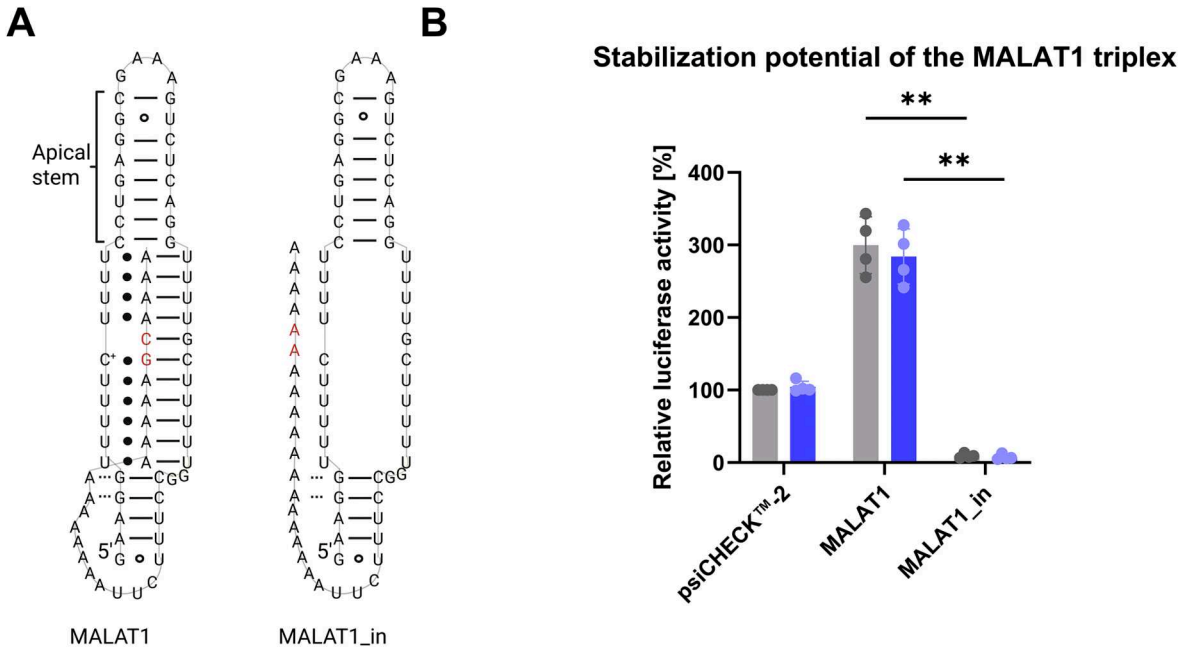

Figure 2. Exploiting the MALAT1 triplex for stabilization of a luciferase reporter gene. (**A**) Sequence and secondary structure of the MALAT1 triplex utilized. In the mutated MALAT1 triplex (MALAT1_in) the C^+·G-C base triple and the C-G duplex were abolished to destabilize triplex formation. "◦" represent non-canonical base pairing and "•" represents Hoogsteen interactions. Lines represent Watson–Crick base pairing and dashed lines A-minor interactions. Created in BioRender; Gommeringer, P. (2026) https://BioRender.com/plhzuir. (**B**) Determination of Renilla luciferase activity after transient transfection with psiCHECK™-2 plasmids containing the MALAT1 triplex or MALAT1_in at the 3′ end of its mRNA. Shown is the relative luciferase activity in the absence (gray) or presence (blue) of 50 μM tetracycline. Renilla luciferase signals are normalized to the activity of the constitutively expressed firefly luciferase encoded on the same vector. The activity of psiCHECK™-2 in the absence of tetracycline has been set to 100%. Error bars represent the standard deviation of the mean values of four independent biological replicates.

Statistical analysis

Statistical analysis was performed in GraphPad Prism version 10.4.1. *P*-values were determined by a two-way analysis of variance (ANOVA) (ns = $P > .05$, * = $P \leq .05$, ** = $P \leq .01$; *** = $P \leq .001$, **** = $P \leq .0001$). Dose-dependency measurements were analyzed using a non-linear curve fit to calculate the EC_{50}. The data were fitted to a sigmoidal dose-response curve using the "[Agonist] vs. response – Three parameters" equation. This model assumes a standard Hill slope of 1.0 and fits the following equation:

$$Y = Y\min + X * \frac{Y\max - Y\min}{\mathrm{EC50} + X}.$$

Results

Assessing the MALAT1 ENE as a riboswitch platform

Both the nuclear NEAT1 and MALAT1 lncRNAs are known to have an extended half-life due to stabilization by RNA triplexes in their 3′-regions, preventing RNase-mediated 3′ to 5′ degradation [38]. Further, they have been shown to stabilize intron-less β-globin mRNA and GFP in the cytoplasm [35, 39]. The stability of triplexes is highly dependent on the flanking duplexes. Hence, we hypothesized that the structure of the RNA triplex MALAT1 ENE would allow us to construct tetracycline-dependent riboswitches by modulating the stability of the adjacent duplexes. First, to assess the stabilizing effect of the triplex in our context, we introduced the MALAT1 ENE core sequence [25] without aptamer (Fig. 2A) directly behind the stop codon of a Renilla luciferase in the dual-luciferase plasmid context (psiCHECK™-2). The 3′ end was matured by a self-cleaving HDV ribozyme instead of a mascRNA, to cleave off the poly-A tail and releasing the transcript with the encoded A-rich stretch at its 3′ end. The HDV ribozyme was chosen for its efficient cleavage rates at its 5′ end [40] and being independent of proteins. As expected, transient transfections showed that the RNA triplex stabilized the transcript and still resulted in efficient protein translation, even with a ribozyme-mediated cleavage of the poly-A tail, showing increased relative luciferase activity of 300.0 ± 39.1% compared to the parental psiCHECK™-2 vector (Fig. 2B). To assess the hypothetical OFF-state of a switch that controls triplex formation, we introduced mutations into the A-rich tract that were reported to destabilize the formation of the triplex [26] (Fig. 2A). Relative luciferase activity dropped to 9.3% for the MALAT1_in construct, which amounts to a 32.3-fold reduced expression compared to the non-mutated construct (Fig. 2B). Independent of this finding, treatment of these controls with 50 μM tetracycline did not significantly alter gene expression. This is important to note since tetracycline has been shown to interact with certain RNA structures [41].

Next, we evaluated the capacity of the MALAT1 ENE to induce gene expression in dependence of a small molecule. We decided to utilize the tetracycline aptamer cb28 minimer [7]. To assess the switching capacity, we connected the aptamer via its P1 stem into the apical stem of the MALAT1 triplex, connected via a so-called communication module (Fig. 3A). We hypothesized that the triplex structure would not form in a cellular environment without formation of an apical stem loop. Upon tetracycline binding, the aptamer is stabilized, and the communication module translates the ligand-induced conformational change of the aptamer onto the triplex.

Downloaded from academic.oup.com/nar/article/54/14/gkag747/8742449 by Deutsches Krebsforschungszentrum user on 18 November 2026

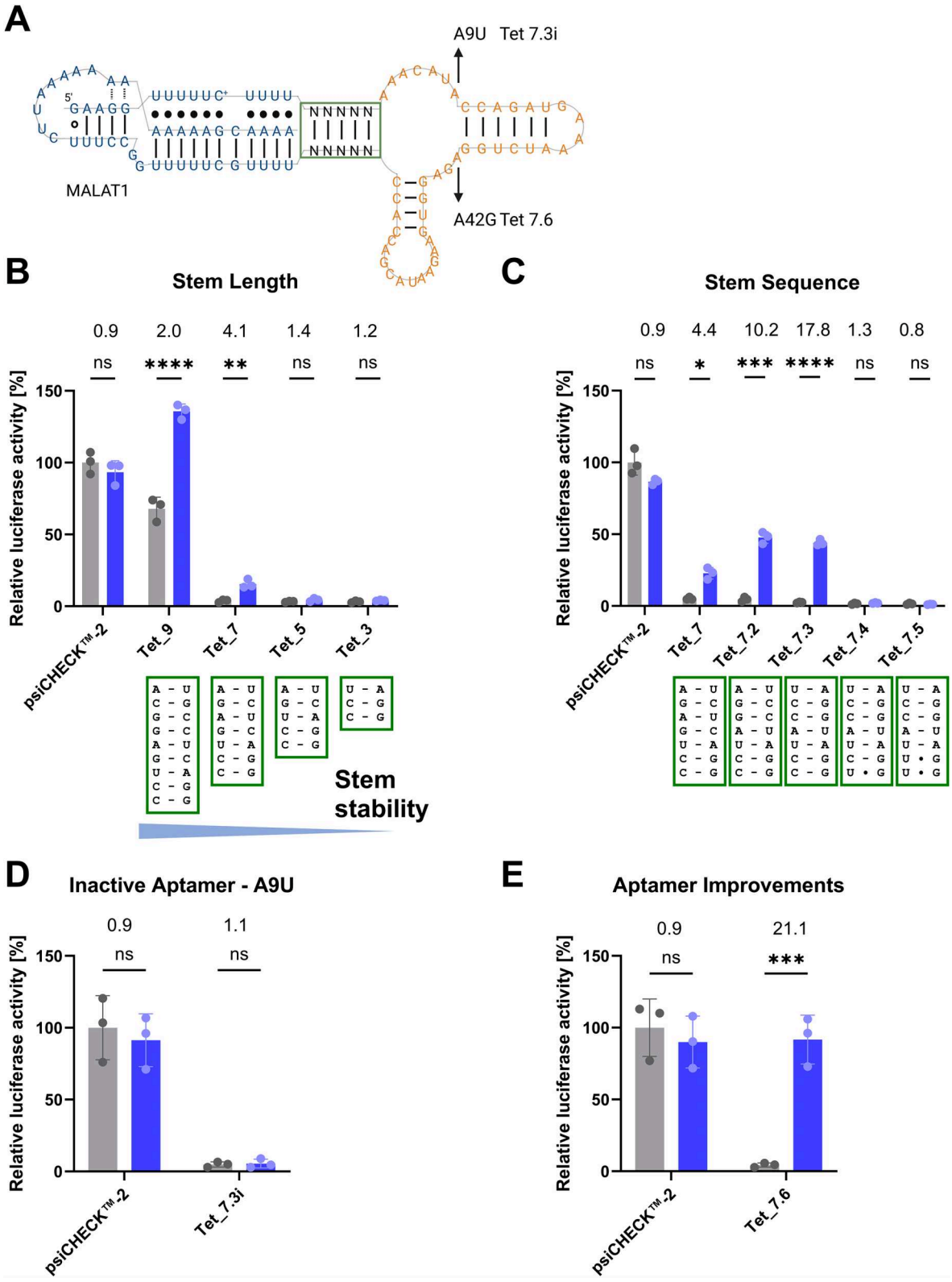

Figure 3. Tetracycline-dependent gene expression via inducible MALAT1 triplex formation. (**A**) Depicted is the sequence and secondary structure of the MALAT1 riboswitch. The triplex is depicted in blue and the aptamer in orange. The communication module is boxed in green. "◦" represent non-canonical base pairing and "•" represents Hoogsteen interactions. Lines represent Watson-Crick base pairing and dashed lines A-minor interactions. Investigated mutations are indicated. Created in BioRender; Gommeringer, P. (2026) https://BioRender.com/m8lj2vp. (**B**, **C**) Determination of triplex-mediated gene expression of Renilla luciferase in the absence (gray) or presence (blue) of 50 μM tetracycline in Hela cells. Respective communication modules are shown beneath (B, C). Determination of triplex-mediated induction of gene expression of Renilla luciferase with (blue) or without (gray) 50 μM tetracycline of the Tet_7.3 switch containing mutations in the aptamer reported to abolish (**D**, Tet_7.3i) or to increase tetracycline binding (**E**, Tet 7.6). Renilla luciferase signals have been normalized to firefly luciferase signals. Uninduced control has been set to 100%. Error bars represent the standard deviation of the mean values of three independent biological replicates. Numbers indicate fold change.

Downloaded from academic.oup.com/nar/article/54/14/gkag747/8742449 by Deutsches Krebsforschungszentrum user on 18 November 2026

Subsequently the triplex would fold and could protect the RNA transcript from RNase-mediated degradation. Thus, ligand-dependent folding of the triplex structure can be engineered by fine-tuning the communication module. Initially, we used the nucleotide sequence of the apical stem used for crystallization and shortened it to 9, 7, 5 or 3 nucleotides (Fig. 3B). Results of transient transfections of plasmids containing switches differing in length of the communication module showed that the riboswitch depends on the stability and length of the communication module. While the construct Tet_9 showed minimal switching efficiency of 2.0-fold with high ON and OFF states, Tet_7 switched 4.1-fold and at a lower absolute expression level (Fig. 3B). Further destabilization of the stem by shortening (Tet_5 and Tet_3) led to basal gene expression and abolished switching. Using rational design approaches, the communication module of seven nucleotides was improved further (Fig. 3C). While introduction of a non-canonical U·G base pair abolished induction of gene expression (Tet_7.4 and Tet_7.5), canonical base pairing led to an increased induction of gene expression to 17.8-fold (Fig. 3C) in the best-performing construct, Tet_7.3.

It is known that the MALAT1 lncRNA is highly overexpressed in cancer cells [42, 43], where the cell environment might favor triplex formation due to lower pH [26]. To further validate our system and to rule out cell-line specific effects, we transiently transfected HEK293 cells. Similar to HeLa cells, MALAT1 ENE was able to stabilize gene expression to 214.8 ± 41.7% whereas a triplex that contained disruptive mutations, MALAT1_in, showed luciferase activity of 9.1 ± 2.3% in HEK293 cells (Supplementary Fig. S2A). A panel of switches led to comparable ON/OFF ratios as in HeLa cells (Supplementary Fig. S2B), suggesting that triplex-mediated riboswitch systems could be applied in a variety of human cell lines. Abolishing tetracycline binding by introduction of the well-known A9U mutation in the aptamer disrupted tetracycline-dependent induction of gene expression in HeLa cells to 4.8 ± 1.8% and 5.4 ± 3.1% without and with 50 μM tetracycline, respectively (Fig. 3D) [18, 44]. Recently, a mutation in the cb28 aptamer, named A42G (Fig. 3A), was shown to increase the fold change in the context of a riboswitch regulating splicing and a poly-A cleavage signal [19]. We introduced the A42G mutation into the triplex switch Tet_7.3 (resulting in Tet_7.6) and demonstrated increased levels of gene expression of 91.6 ± 17.0% while maintaining a low OFF state of 4.3 ± 1.4% in construct Tet_7.6. This further increased the dynamic range to 21-fold (Fig. 3E). To validate whether the mutation would increase the sensitivity of the system towards tetracycline, we investigated the dose-response of the system to its ligand. Introduction of the mutation decreased the EC_{50} from 44 μM to 26 μM tetracycline (Supplementary Fig. S3).

To further investigate the structure-function relationship of the riboswitch beyond the aptamer, which is shown (see Fig. 3D and E), we decided to mutate the A-rich tract (Supplementary Fig. S4A) by introducing the same destabilizing GC to AA mutations (Tet_7.7_Arich) and by deleting the A-rich tract (Tet_7.7_noA). After transfection, we measured relative luciferase signals of 2.7% and 0.1% for Tet_7.7_Arich and Tet_7.7_noA, respectively (Supplementary Fig. S4B).

In summary, these data show that the newly developed platform depends on folding of the communication module induced by an aptamer. The presence of an aptamer does not hinder the folding of the RNA triplex, and its formation can be rendered ligand-dependent and is tunable via rational design approaches.

Triplex-based switches show modularity towards exchanging the RNA triplex and the aptamer

To investigate the modularity of the newly developed triplex platform, the MALAT1 ENE element was exchanged with the NEAT1 triplex [26]. It was chosen due to its high structural resemblance to MALAT1 ENE. Both triplexes use a genetically encoded A-rich stretch and function independently of the poly-A tail. However, the NEAT1 triplex stem is composed of 8 base triples, whereas the MALAT1 triplex has 10 base triples. It is therefore thought to be less stable compared to the MALAT1 triplex. Introducing the NEAT1 ENE into the 3′-UTR of the Renilla luciferase gene directly downstream of the stop codon led to signals of 72.8 ± 18.5% of the psiCHECK™-2 control plasmid, compared to 300.0 ± 39.1% measured beforehand for the MALAT1 triplex (Fig. 2B). Interestingly, introduction of disruptive mutations into the NEAT1 triplex led to much lower gene expression of 0.6 ± 0.2% of Renilla luciferase activity (Fig. 4A), compared to 9.3 ± 3.0% for the MALAT1 ENE (Fig. 2A), resulting in a hypothetical dynamic range of 121. Low basal gene expression is crucial for the generation of potent switches without leaking gene expression. We hypothesized that introducing the communication module that performed best in the MALAT1 context onto the NEAT1 triplex would maintain a high fold change but switch at lower absolute expression levels. Hence, we generated the constructs NEAT1_Tet_7 and NEAT1_Tet_7.3, where the communication module showed promising results in the MALAT1 context and NEAT1_Tet_9 and NEAT1_Tet_8—two constructs having the natural NEAT1 stem sequence as a communication module. Data showed that while NEAT1_Tet_9 and NEAT1_Tet_8 possessed moderate regulatory folds of 2.0 and 3.1, respectively, NEAT1_Tet_7 and NEAT1_Tet_7.3 did not show switching activity and only limited expression of the reporter gene (Fig. 4B). Further improvement of the communication module is hypothesized to increase the switching performance. This led to the hypothesis that the stability of the adjacent duplexes directly influences the stability of the RNA triplex. Accordingly, introducing the natural A·G noncanonical base pair found directly adjacent to the triplex of the natural NEAT1 bases into the MALAT1 context (Tet_7.7) increased the fold change to 25.1 compared to 20.5-fold for Tet_7.6 (Fig. 4C). Introduction of the mutation also lowered absolute gene expression, switching in a range from 0.96 ± 0.2% to 24.0 ± 4.6%.

Although the HDV ribozyme is highly active, cleaves rapidly, and enables the riboswitch to function independently of nuclear proteins—making it well-suited as a maturation platform—we hypothesized that the naturally evolved mascRNA sequence could be equally suitable for certain applications where independence from nuclear enzymes is not required. Hence, we exchanged the HDV ribozyme of Tet_7.2 with the naturally evolved mascRNA, which gets processed via nuclear RNAse P cleavage, as described before, generating Tet_7.2_masc. Luciferase assays showed that insertion of the mascRNA downstream of the triplex did not lead to significant changes in luciferase activity levels with fold changes

Downloaded from academic.oup.com/nar/article/54/14/gkag747/8742449 by Deutsches Krebsforschungszentrum user on 18 November 2026

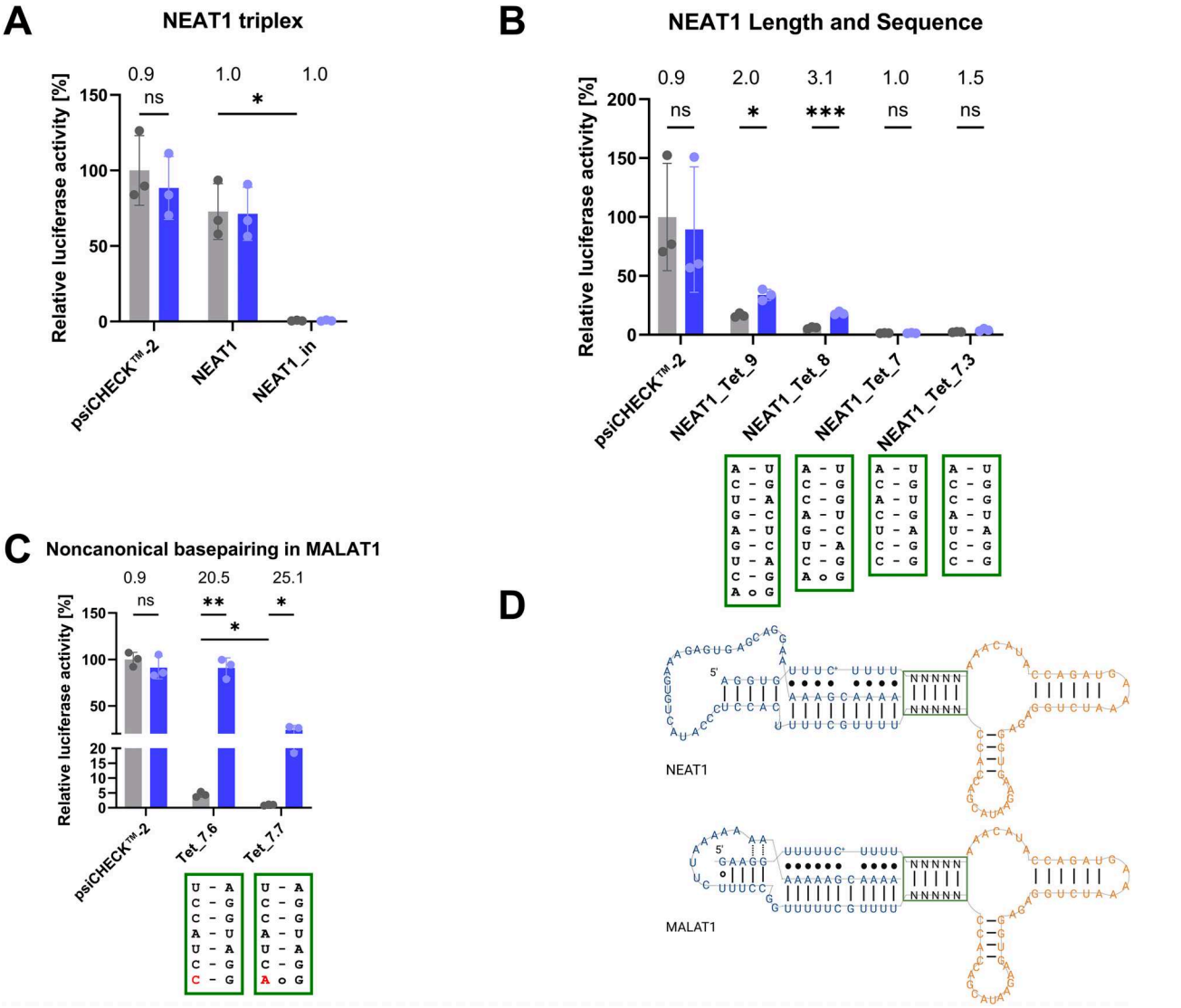

Figure 4. MALAT1 triplex can be exchanged with the NEAT1 triplex and noncanonical base-pairing improves MALAT1 triplex. Determination of triplex-mediated gene expression of Renilla luciferase stabilized by a NEAT1 triplex or a mutated NEAT1 triplex (**A**), regulated by a NEAT1 triplex connected to a tetracycline aptamer with different communication modules (green boxes, **B**), or MALAT1 triplex connected to a tetracycline aptamer with different communication modules (green boxes, **C**), each with (blue) or without (gray) tetracycline. Renilla luciferase activity was normalized to firefly luciferase signals. The uninduced psiCHECK™-2 control has been set to 100%. Error bars represent the standard deviation of the mean values of three independent biological replicates. Numbers indicate fold change. (**D**) Sequence and secondary structure of the NEAT1 riboswitch (up) and MALAT1 riboswitch (down). "◦" represent non-canonical base pairing and "•" represents Hoogsteen interactions. Lines represent Watson–Crick base pairing and dashed lines A-minor interactions. Created in BioRender; Gommeringer, P. (2026) https://BioRender.com/2aznkhy.

of 10.3 and 9.9 for Tet_7.2 and Tet_7.2_masc, respectively (Supplementary Fig. S5), showing that the natural maturation platform can be used as an alternative.

Leaky gene expression is often a limiting factor for *in vivo* application of synthetic riboswitches, especially considering the expression of genes showing systemic toxicity or having narrow therapeutic windows. Furthermore, leaky expression of transgenes can also hamper production of gene therapy vectors [45]. To further validate whether gene expression in the OFF state of our system is due to spontaneous triplex formation or inefficient HDV ribozyme cleavage resulting in polyadenylated transcripts, we introduced degron sequences. Five repeats of the well-known wt1 motif (UAAGUUAU), which has been described to drastically reduce gene expression [35], were introduced downstream of the ribozyme in Tet_7.2 generating the construct Tet_7.2_degron. Since Tet_7.2 still showed an uninduced level of 4.7 ± 1.6%, this construct was thought to be a suitable candidate for reducing the levels of the OFF state. If polyadenylated transcripts were still present and being translated, the degradation sequence motifs would help reduce the Renilla luciferase signals in the OFF state. However, Tet_7.2 and Tet_7.2_degron showed similar fold changes of 10.3 and 8.6 (Supplementary Fig. S6), respectively. Basal gene expression was unaffected, suggesting that basal gene expression is not due to polyadenylated transcripts in the cytoplasm.

Since we were able to exchange the triplex of the system and successfully generated functioning riboswitches after small optimizations, we next investigated whether the aptamer could be exchanged in a modular fashion. The availability of a variety of different small molecule effectors could

Downloaded from academic.oup.com/nar/article/54/14/gkag747/8742449 by Deutsches Krebsforschungszentrum user on 18 November 2026

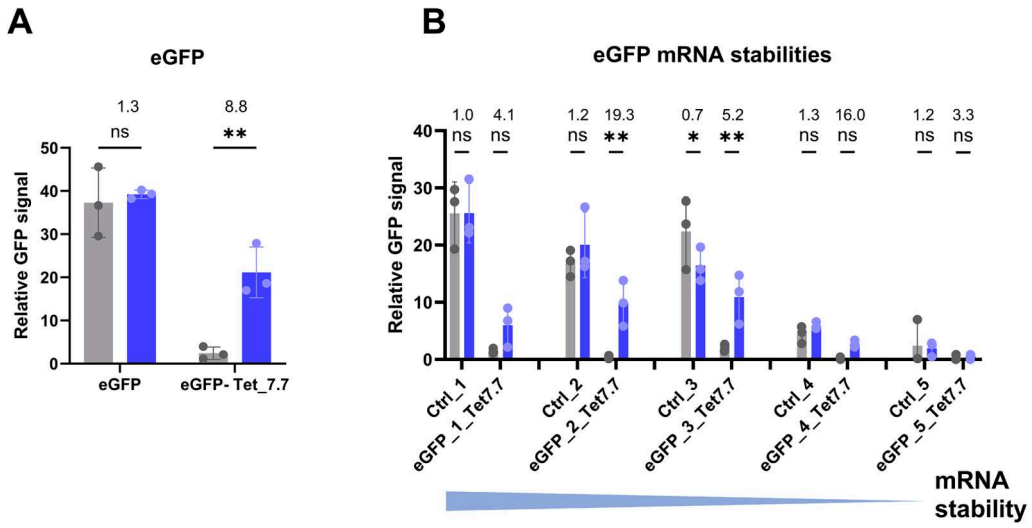

Figure 5. The MALAT1 riboswitch platform can be used to regulate eGFP expression. (**A**) Relative eGFP signal measured in HeLa cells after transient transfection and as determined by fluorescence intensity relative to firefly expression with (blue) or without (gray) 50 μM tetracycline is shown. (**B**) eGFP signals of variants with decreasing mRNA stability from left to right in HeLa cells. Cells were treated with (blue) or without (gray) 50 μM tetracycline. eGFP signal has been normalized to firefly luciferase signal. Error bars represent the standard deviation of the mean values of three independent biological replicates. Numbers indicate fold change.

be beneficial in future applications of the system. For this purpose, we exchanged the tetracycline aptamer with the guanine xpt aptamer [46, 47]. We introduced communication modules with different stem stabilities and varying lengths as carried out with the tetracycline aptamer. With decreasing stability of the communication module, decreasing Renilla luciferase signals were measured, as expected. The riboswitch Gua_L9 with a communication module of 9 base pairs showed 1.7-fold induction of gene expression, while a construct with 3 base pairs, Gua_L3, showed gene induction rates of 2.1-fold (Supplementary Fig. S7). It is important to note that the control showed some induction rate (1.6-fold) due to the inducer molecule itself. The best-performing riboswitch, Gua_L5, led to a moderate fold change of up to 2.6 using 250 μM guanine (Supplementary Fig. S7). Hence, we observed some degree of modularity and hypothesize that the system can generally be optimized for different aptamers.

Triplex-based switches are not dependent on transcript stability but on mRNA coding sequence

mRNAs can be heavily modified post-transcriptionally. For example, m6A modifications as well as protein binding motifs and RNA secondary structures are known to differ between transcripts [48, 49]. To exclude that the MALAT1 triplex switch only functions specifically in the context of Renilla luciferase, we exchanged the ORF to eGFP. Our results showed that it was possible to induce eGFP gene expression up to 8.8-fold (Fig. 5A). Higher expression of eGFP in the uninduced state compared to hRluc reduced the overall switching efficiency. Additionally, the Tet_7.7 construct was introduced 3′ of the firefly luciferase. Only limited ON/OFF ratios of 2.3 were detected for regulation of firefly luciferase (Supplementary Fig. S8), suggesting that the triplex switch needs to be optimized depending on the regulated transgene. To further investigate the ORF dependency of the riboswitch, we took advantage of previously reported eGFP variants that encode the same protein but differ in their mRNA sequences [49].

We hypothesized that the efficiency of the switch is dependent upon differences in mRNA stability resulting from factors such as RNA binding proteins [50, 51], the use of suboptimal codons [52, 53] and the secondary structure [49, 54]. We concluded that the MALAT1 riboswitch could be dependent upon the secondary structure of the mRNA, or codon usage. To further investigate the ORF dependency of the riboswitch, we took advantage of previously reported eGFP variants that encode the same protein but differ in their mRNA sequences. It has been shown before that mRNA secondary structure and codon usage both have an influence on mRNA turnover [49]. Hence, we explored already reported eGFP mRNA variants that encode for the same proteins, however, differ in their relative synonymous codon usages (RSCU) and their minimum free energy (MFE) of folding. Low RSCU represents rare codon usage. RSCU was high for eGFP_1_Tet7.7 and eGFP_3_Tet7.7, low for eGFP_5_Tet7.7 and mid for eGFP_2_Tet7.7 and eGFP_4_Tet7.7. eGFP_1 and eGFP_2 are highly structured (−344 kcal/mol and −346 kcal/mol, respectively). eGFP_3 (−300 kcal/mol) and eGFP_4 (−283 kcal/mol) showed intermediate MFE and eGFP_5 is weakly structured (−209 kcal/mol). Indicated MFEs were calculated using mFold [55] and corresponded to reported values [49]. We hypothesized that the triplex would have a greater impact in stabilizing otherwise highly unstable mRNAs and therefore increase the fold change. We generated five eGFP constructs with a reported stability gradient (Ctrl_1 to Ctrl _5) and the respective constructs containing the Tet_7.7 riboswitch. Transient transfection experiments showed that the controls without a switch behaved as expected, with the signal decreasing in relation to the mRNA stability and codon usage, as reported before. While the construct with the most stabilized mRNA, eGFP_1_Tet7.7, exhibited a ratio of 4.1, we measured a considerably increased fold change of 19.3 and 16.0 for eGFP_2_Tet7.7 and eGFP_4_Tet7.7, respectively (Fig. 5B). Interestingly, eGFP_3_Tet7.7, falling between the previous two, showed an ON/OFF ratio of only 5.2. eGFP_5_Tet7.7 was poorly expressed, and reporter measurements were below the detection limit of the method. Overall, we observed that the

Downloaded from academic.oup.com/nar/article/54/14/gkag747/8742449 by Deutsches Krebsforschungszentrum user on 18 November 2026

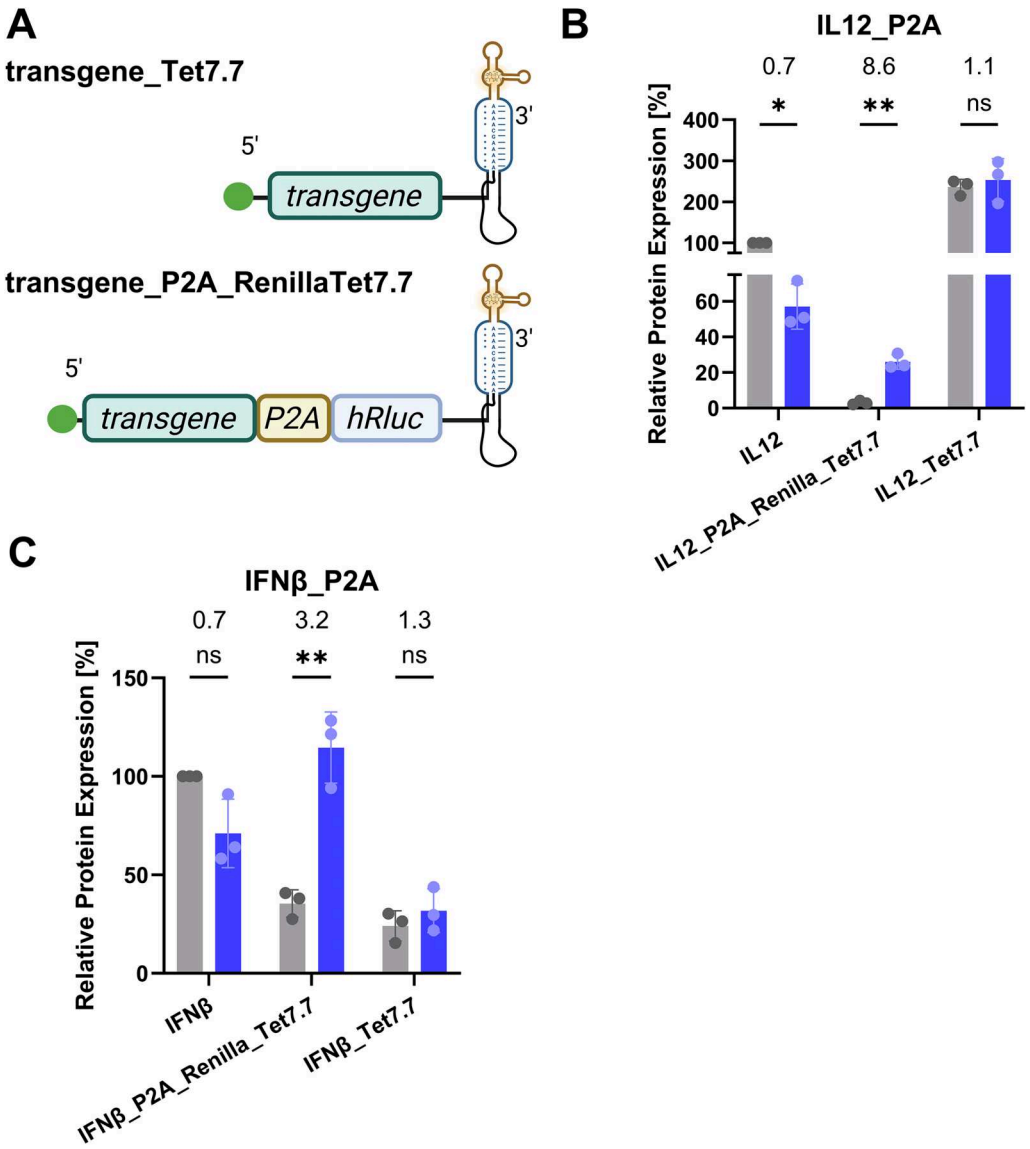

Figure 6. Induction of therapeutic genes. (**A**) Schematic representation of the transgene inserted 5′ of the triplex or 5′ of the renilla luciferase, separated via a P2A sequence. Created in BioRender; Gommeringer, P. (2026) https://BioRender.com/zdb2cpz. (**B**) IL12 levels or (**C**) IFNβ levels 24 h post transfection in HeLa cells treated with (blue) or without (gray) 50 μM tetracycline measured via ELISA. Uninduced control has been set to 100%. Error bars represent the standard deviation of the mean values of three independent biological replicates. Numbers indicate fold change.

MALAT1 riboswitch can regulate different genes and works with mRNAs of varying stabilities. While it seems that intrinsic secondary structure and codon usage seem to have some influence on the triplex riboswitch performance, no clear correlation is observable.

MALAT1-triplex riboswitches can induce gene expression of therapeutic transgenes

To further assess the capacity of the MALAT1 triplex riboswitch to induce gene expression of different therapeutically relevant transgenes, we cloned the triplex switch into the 3′ UTR of murine IL-12 and murine interferon β (see Fig 6A). ELISA data of transient transfection showed that the triplex riboswitch did not induce mIL-12 or mIFNβ expression when placed directly behind the stop codon (Fig. 6B and C). We hypothesized that the Renilla luciferase might have a suitable nucleotide composition and might promote the ability of the riboswitch to induce gene expression. Hence, we connected the mIL-12 and mIFNβ ORF to the Renilla luciferase via a P2A sequence on the same ORF [56] (Fig. 6A). P2A are viral sequences that enable translating of two polypeptides from the same mRNA. The ribosome cannot catalyze peptide bond formation between glycine and proline of the P2A, leading to skipping of bond formation while continuing the translation process leading to expression of two separate proteins (sequence in Supplementary. Table 1). After transient transfection, ELISA data showed induction rates of up to 8.6-fold and 3.2-fold for mIL-12 and mIFNβ, respectively, showing that addition of the Renilla luciferase enables induction of gene expression in this context.

MALAT1-triplex riboswitches can be combined with other riboswitches

It has been shown that the combination of two riboswitch platforms based on a new ASP2905 binding aptamer, namely splicing-based riboswitches and aptazymes, synergize well

Downloaded from academic.oup.com/nar/article/54/14/gkag747/8742449 by Deutsches Krebsforschungszentrum user on 18 November 2026

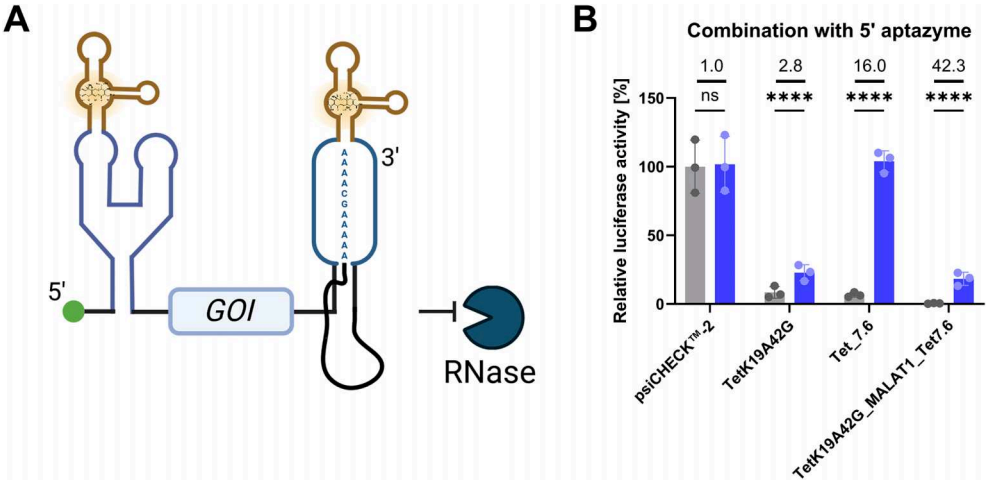

Figure 7. Combination of the MALAT1-based riboswitch with an aptazyme. (**A**) Schematic representation of the combination of the ribozyme and MALAT1-triplex based riboswitches. Created in BioRender; Gommeringer, P. (2026) https://BioRender.com/esz6orv. (**B**) Determination of single and combination riboswitch-mediated gene expression of Renilla luciferase in HeLa cells treated with (blue) or without (gray) 50 μM tetracycline. The triplex switch Tet_7.6 was combined with the aptazyme TetK19A42G in the 5′-UTR. Uninduced control has been set to 100%. Error bars represent the standard deviation of the mean values of three independent biological replicates. Numbers indicate fold change.

[15]. To this end, we investigated the ability of our new triplex riboswitch to function in combination with switches based on other platforms. Since the MALAT1 triplex switch is strictly limited to the 3′-UTR, we combined it with an aptazyme inserted 18-nt upstream of the start codon (Fig. 7A). We used an optimized version of the tetracycline-inducible hammerhead aptazyme TetK19 [9], harboring the previously mentioned A42G mutation in the aptamer. TetK19 has been shown to only moderately induce gene expression in the 5′ UTR [9, 57]. Since it has been shown that highly structured regions in the 5′-UTR, like aptazymes, act as roadblocks to the ribosome and lower the translation rate [58, 59], we combined it with Tet_7.6 as this variant of the triplex switch is characterized by a high absolute level of gene expression. We introduced the aptazyme 18-nt upstream of the start codon. The combination reached fold changes of 42.3 showing an OFF state of 0.4 ± 0.2% and an ON state of 18.3 ± 4.7% (Fig. 7B). The single switches only exhibited fold changes of 2.8 for the aptazyme and 16.0 for Tet_7.6. These data indicate that Tet-dependent MALAT1 triplex riboswitch can be combined to function synergistically with riboswitches placed in the 5′-UTR.

Discussion

Universally applicable genetic switches to induce or repress gene expression are intensively researched in the field of synthetic biology. They are helpful to address basic research questions and might play important roles in the rapidly growing field of gene therapy. Inducible promoters have often been used in the past [60, 61]. However, the foreign transcription factors on which they rely on are inherently immunogenic and require lots of coding space [62]. Additionally, they are dependent on nuclear localization, limiting their application for platforms such as cytoplasmic oncolytic viruses [63, 64]. RNA-based switches are inherently non-immunogenic and require less genetic coding space. Riboswitches that do not depend on nuclear localization have been developed based on occlusion of miRNA target sites and aptazymes. However, while aptazymes only show limited inducibility so far, miRNA-based riboswitches are dependent on the miRNA expression level. Designing riboswitches for mammalian cells remains a challenge and there is still a high need for synthetic riboswitches that show applicability in different modalities of gene delivery systems, pronounced switching performances as well as good compatibility with other switch platforms. Therefore, new designs are needed.

Here, we present a new riboswitch concept, designed to function independently of nuclear proteins. The mechanism relies on the RNA stabilization domains found at the 3′ end of lncRNAs such as MALAT1, also called ENE. It enables translation of mRNAs even in the absence of a poly-A tail [35, 65]. Gene expression is also found to be enhanced compared to constructs harboring a poly-A tail most likely due to longer mRNA half-life [29] as we confirmed with our data. By modulating apical stem formation, we were able to engineer the MALAT1 triplex into a functioning riboswitch. The stem was connected to the P1 stem of the tetracycline binding aptamer cb28 [7]. Via rational design approaches, we were able to identify a suiSupplementary Table Stem composition for the communication module connecting the two elements. MALAT1-based triplex switches with induction rates of up to 25-fold were generated. This is a significant improvement since other tetracycline-inducible systems that do not rely on nuclear localization have shown fold inductions of 4.8 and 5.5 for a hammerhead-based aptazyme [9] and a pistol-based aptazyme [11], respectively. Further, a riboswitch based on masking of the miRNA target site 21 showed a regulatory fold change of 20.0 [17].

To facilitate the design of new expression systems and therapeutic applications, maintaining flexibility is essential. Aptazymes have been shown to function using different ribozyme platforms [9, 11] as well as different aptamers [66, 67]. Splicing-based riboswitches have shown a similar degree of modularity [13–15, 68]. To assess modularity in our system, the HDV ribozyme in the maturation platform was replaced with the natural mascRNA sequence, the MALAT1 triplex with the NEAT1 triplex, and the tetracycline aptamer with the guanine xpt aptamer. Although induction rates decreased when exchanging the triplex and aptamer the constructs main-

Downloaded from academic.oup.com/nar/article/54/14/gkag747/8742449 by Deutsches Krebsforschungszentrum user on 18 November 2026

tained inducibility. Optimization of the communication module could increase the fold change.

The MALAT1 riboswitch showed high fold changes using the reporter genes eGFP and Renilla luciferase. However, firefly luciferase only showed induction of 2.3-fold (Supplementary Fig. S8). We observed that direct switching of mIL12 and mIFNβ did not lead to an increase in fold induction upon treatment with 50 μM tetracycline. However, when those transcripts were linked via a P2A sequence to the Renilla luciferase, fold induction rates of 8.6-fold and 3.2-fold were measured for mIL12 and mIFNβ, respectively. The difference in gene induction rates could be due to differences in $3' \rightarrow 5'$ degradation by the exosome compared to $5' \rightarrow 3'$ degradation by other pathways as described for the lncRNA MALAT1 [69]. RNA degradation is a highly complex process. Both pathways are thought to be influenced by the nucleotide composition of the RNA. The data also show that the mRNA sequence itself has an impact on fold induction. Further investigation needs to be conducted to test this hypothesis and to improve inducibility of the triplex switch for alternative transgenes.

While the riboswitch retained inducibility in most contexts, exchange of the aptamer, the triplex and the coding sequence led to reduction in dynamic ranges that we could partially restore by modulation of the communication module or the coding sequence. As such, we laid the groundwork for further exploration and optimization of the triplex riboswitch design. Especially our findings regarding the switch performance depending on the coding sequence need to be investigated further.

Inducible gene expression systems can be used in a therapeutic context as well as to induce gene expression for protein production. In both cases, leaky gene expression should be avoided to either increase protein yields or optimize therapeutic outcomes and avoid toxic side effects [70]. It was shown before that combination of two riboswitch platforms leads to tight control over gene expression [15]. We showed that the MALAT1 triplex switch in combination with an aptazyme was able to reduce background expression of the Renilla luciferase to 0.4% while retaining a high ON-state. Hence, the MALAT1 triplex switch is a suitable candidate to control gene expression with low leakiness.

Taken together, we were able to establish the stability elements of RNA-triplexes as new platforms for engineering of RNA-based genetic ON switches that function in the cytoplasm and are completely independent of nuclear mechanisms. Independence of nuclear proteins is highly relevant for new therapeutic approaches, like self-amplifying mRNA or for oncolytic viruses, using strictly cytoplasmic viruses, where aptazymes have already been shown to regulate virus replication [63, 64, 71, 72]. Overall, the triplex-based riboswitch platform represents a promising new option for inducing expression in gene therapy platforms.

Acknowledgements

We want to thank Astrid Joachimi, Stefanie Sawall, Jessica Genz, Milena Barf, and Birgit Hoyler for excellent technical support. We also thank all other valuable members of our research team at the University of Konstanz and at the Clinical Cooperation Unit Virotherapy at the German Cancer Research Centre (DKFZ) for their valuable feedback and enduring support. We thank the anonymous reviewers for their suggestions and improvements. Figures were created in BioRender and can be found using the links in the legends (graphical abstract: https://BioRender.com/da0rr9p), licensed under CC BY 4.0.

Author contributions: Pierre Gommeringer: Conceptualization, Experimentation, Analysis, Writing—original draft & editing. Elisabeth Müller: Experimentation, Analysis, Writing—review & editing. Sila Köse: Experimentation, Analysis, Writing—review & editing. Laura Kayser: Writing—review & editing. Mathias F. Leber: Writing—review & editing. Guy Ungerechts: Writing—review & editing. Dirk M. Nettelbeck: Analysis, Writing—review & editing. Jörg S. Hartig: Conceptualization, Analysis, Writing—review & editing.

Supplementary data

Supplementary data is available at NAR online.

Conflict of interest

G.U. is founder, CMO, CSO and board member of CanVirex AG that filed a patent application for use of triplex-based riboswitches. P.G. and J.S.H. are the inventors on that patent (PCT/EP2025/087838).

Funding

This project was supported by the German Cancer Aid (Deutsche Krebshilfe) under grant number 70114315 and 70114400 (to D.M.N., J.S.H., and G.U.). Funding to pay the Open Access publication charges for this article was provided by University of Konstanz.

Data availability

The data underlying this article are available in the article and in its online supplementary material.

References

1. Tickner ZJ, Farzan M. Riboswitches for controlled expression of therapeutic transgenes delivered by adeno-associated viral vectors. *Pharmaceuticals* 2021;14:554.
2. Breaker RR. Riboswitches and translation control. *Cold Spring Harb Perspect Biol* 2018;10:a032797. https://doi.org/10.1101/cshperspect.a032797
3. Chang AL, Wolf JJ, Smolke CD. Synthetic RNA switches as a tool for temporal and spatial control over gene expression. *Curr Opin Biotechnol* 2012;23:679–88. https://doi.org/10.1016/j.copbio.2012.01.005
4. Kraus L, Duchardt-Ferner E, Bräuchle E *et al.* Development of a novel tobramycin dependent riboswitch. *Nucleic Acids Res* 2023;51:11375–85. https://doi.org/10.1093/nar/gkad767
5. Kraus L, Suess B. RNA capture-SELEX on streptavidin magnetic beads. *Methods Mol Biol* 2023;2570:63–71.
6. Kramat J, Suess B. Efficient method to identify synthetic riboswitches using RNA-based capture-SELEX combined with *in vivo* screening. *Methods Mol Biol* 2022;2518:157–77.
7. Berens C, Thain A, Schroeder R. A tetracycline-binding RNA aptamer. *Bioorg Med Chem* 2001;9:2549–56. https://doi.org/10.1016/S0968-0896(01)00063-3
8. Suess B, Hanson S, Berens C *et al.* Conditional gene expression by controlling translation with tetracycline-binding aptamers. *Nucleic Acids Res* 2003;31:1853–8. https://doi.org/10.1093/nar/gkg285

Downloaded from academic.oup.com/nar/article/54/14/gkag747/8742449 by Deutsches Krebsforschungszentrum user on 18 November 2026

9. Beilstein K, Wittmann A, Grez M *et al.* Conditional control of mammalian gene expression by tetracycline-dependent hammerhead ribozymes. *ACS Synth Biol* 2015;4:526–34. https://doi.org/10.1021/sb500270h
10. Mustafina K, Fukunaga K, Yokobayashi Y. Design of mammalian ON-riboswitches based on tandemly fused aptamer and ribozyme. *ACS Synth Biol* 2020;9:19–25. https://doi.org/10.1021/acssynbio.9b00371
11. Mustafina K, Nomura Y, Rotrattanadumrong R *et al.* Circularly-permuted pistol ribozyme: a synthetic ribozyme scaffold for mammalian riboswitches. *ACS Synth Biol* 2021;10:2040–8. https://doi.org/10.1021/acssynbio.1c00213
12. Felletti M, Hartig JS. Ligand-dependent ribozymes. *Wiley Interdiscip Rev RNA* 2017;8:e1395. https://doi.org/10.1002/wrna.1395
13. Finke M, Brecht D, Stifel J *et al.* Efficient splicing-based RNA regulators for tetracycline-inducible gene expression in human cell culture and C. elegans. *Nucleic Acids Res* 2021;49:e71. https://doi.org/10.1093/nar/gkab233
14. Nomura Y, Kim N, Zhu B *et al.* Optimization of exon-skipping riboswitches and their applications to control mammalian cell fate. *ACS Synth Biol* 2024;13:3246–55. https://doi.org/10.1021/acssynbio.4c00295
15. Fukunaga K, Dhamodharan V, Miyahira N *et al.* Small-molecule aptamer for regulating RNA functions in mammalian cells and animals. *J Am Chem Soc* 2023;145:7820–8. https://doi.org/10.1021/jacs.2c12332
16. Vogel M, Weigand JE, Kluge B *et al.* A small, portable RNA device for the control of exon skipping in mammalian cells. *Nucleic Acids Res* 2018;46:e48. https://doi.org/10.1093/nar/gky062
17. Mou H, Zhong G, Gardner MR *et al.* Conditional regulation of gene expression by ligand-induced occlusion of a microRNA target sequence. *Mol Ther* 2018;26:1277–86. https://doi.org/10.1016/j.ymthe.2018.02.021
18. Spöring M, Boneberg R, Hartig JS. Aptamer-mediated control of polyadenylation for gene expression regulation in mammalian cells. *ACS Synth Biol* 2020;9:3008–18
19. Luo L, Jea JDY, Wang Y *et al.* Control of mammalian gene expression by modulation of polyA signal cleavage at 5′ UTR. *Nat Biotechnol* 2024;42:1454–66. https://doi.org/10.1038/s41587-023-01989-0
20. Wu M, Xu G, Han C *et al.* lncRNA SLERT controls phase separation of FC/DFCs to facilitate Pol I transcription. *Science* 2021;373:547–55. https://doi.org/10.1126/science.abf6582
21. Yamazaki T, Souquere S, Chujo T *et al.* Functional domains of NEAT1 architectural lncRNA induce paraspeckle assembly through phase separation. *Mol Cell* 2018;70:1038–53.e7. https://doi.org/10.1016/j.molcel.2018.05.019
22. Wang H, Zheng X, Jin J *et al.* LncRNA MALAT1 silencing protects against cerebral ischemia-reperfusion injury through miR-145 to regulate AQP4. *J Biomed Sci* 2020;27:40. https://doi.org/10.1186/s12929-020-00635-0
23. Hutchinson JN, Ensminger AW, Clemson CM *et al.* A screen for nuclear transcripts identifies two linked noncoding RNAs associated with SC35 splicing domains. *Bmc Genomics [Electronic Resource]* 2007;8:39. https://doi.org/10.1186/1471-2164-8-39
24. Goyal B, Yadav SRM, Awasthee N *et al.* Diagnostic, prognostic, and therapeutic significance of long non-coding RNA MALAT1 in cancer. *Biochim Biophys Acta Rev Cancer* 2021;1875:188502.
25. Brown JA, Bulkley D, Wang J *et al.* Structural insights into the stabilization of MALAT1 noncoding RNA by a bipartite triple helix. *Nat Struct Mol Biol* 2014;21:633–40. https://doi.org/10.1038/nsmb.2844
26. Brown JA, Valenstein ML, Yario TA *et al.* Formation of triple-helical structures by the 3′-end sequences of MALAT1 and MENβ noncoding RNAs. *Proc Natl Acad Sci USA* 2012;109:19202–7. https://doi.org/10.1073/pnas.1217338109
27. Wilusz JE, Freier SM, Spector DL. 3′ end processing of a long nuclear-retained noncoding RNA yields a tRNA-like cytoplasmic RNA. *Cell* 2008;135:919–32. https://doi.org/10.1016/j.cell.2008.10.012
28. Mitton-Fry RM, DeGregorio SJ, Wang J *et al.* Poly(A) tail recognition by a viral RNA element through assembly of a triple helix. *Science* 2010;330:1244–7. https://doi.org/10.1126/science.1195858
29. Wilusz JE, JnBaptiste CK, Lu LY *et al.* A triple helix stabilizes the 3′ ends of long noncoding RNAs that lack poly(A) tails. *Genes Dev* 2012;26:2392–407. https://doi.org/10.1101/gad.204438.112
30. Tycowski KT, Shu M-D, Steitz JA. Myriad triple-helix-forming structures in the transposable element RNAs of plants and fungi. *Cell Rep* 2016;15:1266–76. https://doi.org/10.1016/j.celrep.2016.04.010
31. Zhang B, Mao YS, Diermeier SD *et al.* Identification and characterization of a class of MALAT1-like genomic loci. *Cell Rep* 2017;19:1723–38. https://doi.org/10.1016/j.celrep.2017.05.006
32. Torabi S-F, Vaidya AT, Tycowski KT *et al.* RNA stabilization by a poly(A) tail 3′-end binding pocket and other modes of poly(A)–RNA interaction. *Science* 2021;371:eabe6523. https://doi.org/10.1126/science.abe6523
33. Yonkunas MJ, Baird NJ. A highly ordered, nonprotective MALAT1 ENE structure is adopted prior to triplex formation. *RNA* 2019;25:975–84. https://doi.org/10.1261/rna.069906.118
34. Ageeli AA, McGovern-Gooch KR, Kaminska MM *et al.* Finely tuned conformational dynamics regulate the protective function of the lncRNA MALAT1 triple helix. *Nucleic Acids Res* 2019;47:1468–81. https://doi.org/10.1093/nar/gky1171
35. DiAndreth B, Wauford N, Hu E *et al.* PERSIST platform provides programmable RNA regulation using CRISPR endoRNases. *Nat Commun* 2022;13:2582. https://doi.org/10.1038/s41467-022-30172-3
36. Weick E-M, Lima CD. RNA helicases are hubs that orchestrate exosome-dependent 3′–5′ decay. *Curr Opin Struct Biol* 2021;67:86–94. https://doi.org/10.1016/j.sbi.2020.09.010
37. Lieschke GJ, Rao PK, Gately MK *et al.* Bioactive murine and human interleukin-12 fusion proteins which retain antitumor activity *in vivo*. *Nat Biotechnol* 1997;15:35–40. https://doi.org/10.1038/nbt0197-35
38. Tani H, Nakamura Y, Ijiri K *et al.* Stability of MALAT-1, a nuclear long non-coding RNA in mammalian cells, varies in various cancer cells. *Drug Discov Ther* 2010;4:235–9.
39. Brown JA, Steitz JA. Intronless β-globin reporter: a tool for studying nuclear RNA stability elements. *Methods Mol Biol* 2016;1428:77–92.
40. Kläge D, Müller E, Hartig JS. A comparative survey of the influence of small self-cleaving ribozymes on gene expression in human cell culture. *RNA Biol* 2024;21:1–11
41. Garner AL, Lorenz DA, Sandoval J *et al.* Tetracyclines as inhibitors of pre-microRNA maturation: a disconnection between RNA binding and inhibition. *ACS Med Chem Lett* 2019;10:816–21. https://doi.org/10.1021/acsmedchemlett.9b00091
42. Mishra A, Mishra S. Metastasis-associated lung adenocarcinoma transcript 1 (MALAT1) lncRNA conformational dynamics in complex with RNA-binding protein with serine-rich domain 1 (RNPS1) in the pan-cancer splicing and gene expression. *ACS omega* 2024;9:42212–26. https://doi.org/10.1021/acsomega.4c04467
43. Zhang Y, Xu Y, Qiu G *et al.* METTL3 mediated MALAT1 m6A modification promotes proliferation and metastasis in osteosarcoma cells. *Mol Biotechnol* 2024;66:3538–48. https://doi.org/10.1007/s12033-023-00953-2
44. Xiao H, Edwards TE, Ferré-D'Amaré AR. Structural basis for specific, high-affinity tetracycline binding by an *in vitro* evolved aptamer and artificial riboswitch. *Chem Biol* 2008;15:1125–37. https://doi.org/10.1016/j.chembiol.2008.09.004
45. Strobel B, Klauser B, Hartig JS *et al.* Riboswitch-mediated attenuation of transgene cytotoxicity increases adeno-associated virus vector yields in HEK-293 cells. *Mol Ther* 2015;23:1582–91. https://doi.org/10.1038/mt.2015.123

Downloaded from academic.oup.com/nar/article/54/14/gkag747/8742449 by Deutsches Krebsforschungszentrum user on 18 November 2026

46. Batey RT, Gilbert SD, Montange RK. Structure of a natural guanine-responsive riboswitch complexed with the metabolite hypoxanthine. *Nature* 2004;432:411–5. https://doi.org/10.1038/nature03037
47. Brenner MD, Scanlan MS, Nahas MK *et al.* Multivector fluorescence analysis of the xpt guanine riboswitch aptamer domain and the conformational role of guanine. *Biochemistry* 2010;49:1596–605. https://doi.org/10.1021/bi9019912
48. Schievelbein MJ, Resende C, Glennon MM *et al.* Global RNA modifications to the MALAT1 triple helix differentially affect thermostability and weaken binding to METTL16. *J Biol Chem* 2024;300:105548. https://doi.org/10.1016/j.jbc.2023.105548
49. Mauger DM, Cabral BJ, Presnyak V *et al.* mRNA structure regulates protein expression through changes in functional half-life. *Proc Natl Acad Sci USA* 2019; 116:24075–83.
50. Ge Z, Quek BL, Beemon KL *et al.* Polypyrimidine tract binding protein 1 protects mRNAs from recognition by the nonsense-mediated mRNA decay pathway. *eLife* 2016;5:e11155. https://doi.org/10.7554/eLife.11155
51. Chenette DM, Cadwallader AB, Antwine TL *et al.* Targeted mRNA decay by RNA binding protein AUF1 regulates adult muscle stem cell fate, promoting skeletal muscle integrity. *Cell Rep* 2016;16:1379–90. https://doi.org/10.1016/j.celrep.2016.06.095
52. Morris C, Cluet D, Ricci EP. Ribosome dynamics and mRNA turnover, a complex relationship under constant cellular scrutiny. *Wiley Interdiscip Rev RNA* 2021;12:e1658. https://doi.org/10.1002/wrna.1658
53. Zhu X, Cruz VE, Zhang H *et al.* Specific tRNAs promote mRNA decay by recruiting the CCR4-NOT complex to translating ribosomes. *Science* 2024;386:eadq8587. https://doi.org/10.1126/science.adq8587
54. Mortimer SA, Kidwell MA, Doudna JA. Insights into RNA structure and function from genome-wide studies. *Nat Rev Genet* 2014;15:469–79. https://doi.org/10.1038/nrg3681
55. Zuker M. Mfold web server for nucleic acid folding and hybridization prediction. *Nucleic Acids Res* 2003;31:3406–15. https://doi.org/10.1093/nar/gkg595
56. Liu Z, Chen O, Wall JBJ *et al.* Systematic comparison of 2A peptides for cloning multi-genes in a polycistronic vector. *Sci Rep* 2017;7:2193. https://doi.org/10.1038/s41598-017-02460-2
57. Strobel B, Düchs MJ, Blazevic D *et al.* A small-molecule-responsive riboswitch enables conditional induction of viral vector-mediated gene expression in mice. *ACS Synth Biol* 2020;9:1292–305. https://doi.org/10.1021/acssynbio.9b00410
58. Werstuck G, Green MR. Controlling gene expression in living cells through small molecule–RNA interactions. *Science* 1998;282:296–8. https://doi.org/10.1126/science.282.5387.296
59. Leppek K, Das R, Barna M. Functional 5′ UTR mRNA structures in eukaryotic translation regulation and how to find them. *Nat Rev Mol Cell Biol* 2018;19:158–74. https://doi.org/10.1038/nrm.2017.103
60. Das AT, Tenenbaum L, Berkhout B. Tet-on systems for doxycycline-inducible gene expression. *CGT* 2016;16:156–67. https://doi.org/10.2174/1566523216666160524144041
61. Azad T, Rezaei R, Singaravelu R *et al.* Synthetic virology approaches to improve the safety and efficacy of oncolytic virus therapies. *Nat Commun* 2023;14:3035. https://doi.org/10.1038/s41467-023-38651-x .
62. Siddiqui M, Tous C, Wong WW. Small molecule-inducible gene regulatory systems in mammalian cells: progress and design principles. *Curr Opin Biotechnol* 2022;78:102823. https://doi.org/10.1016/j.copbio.2022.102823
63. Ketzer P, Haas SF, Engelhardt S *et al.* Synthetic riboswitches for external regulation of genes transferred by replication-deficient and oncolytic adenoviruses. *Nucleic Acids Res* 2012;40:e167. https://doi.org/10.1093/nar/gks734
64. Ketzer P, Kaufmann JK, Engelhardt S *et al.* Artificial riboswitches for gene expression and replication control of DNA and RNA viruses. *Proc Natl Acad Sci USA* 2014; 111:E554–62.
65. Che R, Panah M, Mirani B *et al.* Identification of human pathways acting on nuclear non-coding RNAs using the Mirror forward genetic approach. *Nat Commun* 2025;16:4741. https://doi.org/10.1038/s41467-025-59998-3
66. Sack M, Stifel J, Kreft SG *et al.* Neomycin-dependent hammerhead ribozymes for the direct control of gene expression in Saccharomyces cerevisiae. *Methods* 2019;161:35–40. https://doi.org/10.1016/j.ymeth.2019.01.004
67. Strobel B, Spöring M, Klein H *et al.* High-throughput identification of synthetic riboswitches by barcode-free amplicon-sequencing in human cells. *Nat Commun* 2020;11:714. https://doi.org/10.1038/s41467-020-14491-x
68. Hedwig V, Spöring M, Ottlinger J *et al.* Engineering oxypurinol-responsive riboswitches based on bacterial xanthine aptamers for gene expression control in mammalian cell culture. *Nucleic Acids Res* 2025;53:gkae1189. https://doi.org/10.1093/nar/gkae1189
69. Tuck AC, Rankova A, Arpat AB *et al.* Mammalian RNA decay pathways are highly specialized and widely linked to translation. *Mol Cell* 2020;77:1222–36.e13. https://doi.org/10.1016/j.molcel.2020.01.007
70. Valenzuela-Cardenas M, Fisher C, Bartee MY *et al.* IL-12-mediated toxicity from localized oncolytic virotherapy can be reduced using systemic TNF blockade. *Mol Ther Oncol* 2024;32:200866.
71. Takahashi K, Yokobayashi Y. Reversible gene regulation in mammalian cells using riboswitch-engineered vesicular stomatitis virus vector. *ACS Synth Biol* 2019;8:1976–82. https://doi.org/10.1021/acssynbio.9b00177
72. Kim N, Yokobayashi Y. Novel RNA viral vectors for chemically regulated gene expression in embryonic stem cells. *ACS Synth Biol* 2021;10:2959–67. https://doi.org/10.1021/acssynbio.1c00214

Received: December 23, 2025. **Revised:** July 6, 2026. **Accepted:** July 8, 2026
© The Author(s) 2026. Published by Oxford University Press.
This is an Open Access article distributed under the terms of the Creative Commons Attribution-NonCommercial License (https://creativecommons.org/licenses/by-nc/4.0/), which permits non-commercial re-use, distribution, and reproduction in any medium, provided the original work is properly cited. For commercial re-use, please contact reprints@oup.com for reprints and translation rights for reprints. All other permissions can be obtained through our RightsLink service via the Permissions link on the article page on our site—for further information please contact journals.permissions@oup.com.

Downloaded from academic.oup.com/nar/article/54/14/gkag747/8742449 by Deutsches Krebsforschungszentrum user on 18 November 2026